2022 IMEKO TC-4 International Conference on
Metrology for Archaeology and Cultural Heritage
University of Calabria, Italy, October 19-21, 2022

Multi-technique characterization of colored gem tourmalines

Roberta Somma[1,†], Giuseppe Paladini[1,†,*], Sebastiano Ettore Spoto[1], Francesco Caridi[1], Vincenza Crupi[1], Monica Interdonato[1], Valentina Venuti[1]

[1] Department of Mathematical and Computer Sciences, Physical Sciences and Earth Sciences,
University of Messina, Viale Ferdinando Stagno D'Alcontres 31, I-98166 Messina, Italy,
*rsomma@unime.it, gpaladini@unime.it (*corresponding author), sebastianoettore@gmail.com,*
fcaridi@unime.it, vcrupi@unime.it, monica.interdonato@unime.it, vvenuti@unime.it
[†] First author

***Abstract* – A preliminary investigation was carried out on two different colored tourmalines (TMs), sourced by the Mineral and Gem collection of the Messina University (Messina, Italy). The employment of µ-Raman spectroscopy allowed to unambiguously recognize the mineral sub-group these species belong to, starting from the molecular composition. Through X-ray fluorescence spectroscopy (XRF), the elemental composition of the studied gemstones was achieved, identifying the chromophores responsible for the observed colorations. The obtained results allowed to define the mineral "fingerprinting" and get insights into the crystallization history of the TM host rock and the *criteria* according to which TMs exhibit a particular color.**

I. INTRODUCTION

Tourmalines (TMs) are complex borosilicate minerals with the idealized chemical formula $XY_3Z_6(T_6O_{18})(BO_3)_3V_3W$. They crystallize in the hexagonal crystal family and originate in a wide range of geological environments. They are commonly referred to as a mineral *supergroup,* which comprises, to date, 33 different species approved by the *International Mineralogical Association's Commission on New Minerals, Nomenclature, and Classification*.

The crystal unit of TMs, which belongs to the space-group *R3m* (C^5_{3v}), consists of a lower layer that contains a ditrigonal 6-membered ring of corner-sharing TO_4 tetrahedra (commonly occupied by Si^{4+} ($[Si_6O_{18}]^{12-}$)), with a W- and X-site placed above and below its center, and an upper layer holding a cluster of 3 and 6 non-equivalent Y-site and Z-site octahedra, respectively. Both layers are oriented perpendicular to the *c*-axis of the Bravais unit cell, which runs along the crystals' elongated direction, giving rise to a strong anisotropy along such direction. This property provides tourmalines different direction-related physical/chemical properties, including pyroelectricity and piezoelectricity. The structure is completed by the presence of triangular $[BO_3]^{3-}$ ortho-groups placed between TO_4 tetrahedral rings and of V-sites (usually occupied by OH^- or O^{2-}) shared between one YO_6 and two ZO_6 octahedra.

The name tourmaline originates from the Sinhalese language and means a thousand colors. Due to their extraordinary transparency and brilliance, TMs are considered medium/high-grade gemstones highly demanded by collectors and customers as this mineral can show a variety of hues, tones, and color combinations. Color may be strongly variable along with the directions parallel and orthogonal to the *c*-axis; moreover, due to its typical strong pleochroism, the cut type may be crucial in exalting optical features of TMs. Nowadays, most colored gem-quality TMs are mined in Brazil, Africa, the U.S.A., and Russia. To date, the mechanisms determining the color in TMs are partially unknown [1]. Although the color in TMs is not species-specific, green, red, blue, brown, pink, and even colorless, TMs can be recognized, with color changes as primary due to variations in the chemical composition and geological context. Moreover, TMs can exhibit extremely convoluted *chemical zoning*, which results in quite rare bi-colored TMs (i.e., *watermelon* TMs) whose coloration typically varies, along the *c*-axis, from pinkish to greenish nuances.

In this framework, the possibility to discriminate a specific variety of TMs (sub-group) through the employment of a combined approach involving physical/chemical analyses not only plays a fundamental role in a more profound knowledge of the TM host rock but also could get insights on the *criteria* according to which a tourmaline exhibits a particular color rather than others. The different varieties of tourmaline minerals may be distinguished under the petrographic microscope, considering the refractive indices or birefringence [2]. Notwithstanding, in the case of tourmaline gemstones, it is not possible to damage the sample with invasive techniques and consequently Raman spectroscopy and XRF analyses may be very useful to characterize their composition and ascertain if gemstones are authentic.

Based on the considerations above, a preliminary µ-

Raman and X-ray fluorescence (XRF) spectroscopy non-invasive investigation on two selected TMs, owned by the Mineral and Gem collection of the Messina University (Messina, Italy) was carried out. μ-Raman spectroscopy was adopted to primarily identify the mineral sub-group to which these species belong, trying to correlate the observed μ-Raman band positions to possible cation substitutions within the TM tetrahedral/octahedral sites. XRF spectroscopy allowed identifying the elemental composition of the studied gems, allowing for identifying the chromophore element responsible for the observed coloration.

II. MATERIALS AND METHODS

A. Materials

Two TMs samples TM1 and TM2 were analysed in this study (Fig. 1). Such TMs, sourced from the Mineral and Gem collection of the Messina University (Messina, Italy), are conserved as historical samples dating back to the early twentieth century, which is so significant for cultural heritage.

Fig. 1. Stereomicroscope photographs of the two investigated samples. The direction of the c-axis is also indicated.

B. Methods

μ-Raman measurements were collected by a portable “BTR111MiniRam™” (BW&TEK Inc) spectrometer, working with a 785 nm (diode laser) excitation wavelength and a thermoelectric cooled charge-coupled device (CCD) detector. The system was equipped with a BAC151B Raman microscope. The laser spot was focused on the tourmaline surface through a 40x objective, which guaranteed a working distance of 3.98 mm and a laser beam spot size of 50 μm. The maximum power at the samples was ~ 90 mW. Spectra were registered between 60 and 3150 cm^{-1}, with an acquisition time of 40 s and a resolution of 8 cm-1, by accumulating 32 scans to increase the signal–to–noise ratio. Spectra are the average of 5 different measurements exhibiting similar profiles collected with the incident and scattered light oriented perpendicularly to the *c*-axis direction.

XRF measurements were performed through a portable XRF analyzer “alpha 4000” (Innov–X system) equipped with a tantalum (Ta) anode X-ray tube excitation source and a Si PIN diode with an active area of 170 mm^2. The instrument allowed the detection of chemical elements with an atomic number (Z) between phosphorus and lead. Two sequential tests were carried out on each sample: the first run with the operating condition of 40 kV and 7 μA and the second one with 15 kV and 5 μA, for a total collection time of 120 s. The calibration was carried out by the *soil LEAP* (Light Element Analysis Program) *II* in-house procedure. It was verified using alloy-certified reference materials produced by Analytical Reference Materials International. The statistics of the measured spectra was improved by collecting the XRF signal for 60 s per run.

III. GEOLOGICAL BACKGROUND

Tourmalines typically belong to the paragenesis of granitic pegmatites, pneumatolytic veins, and granites. These borosilicates may be also found in metamorphic rocks due to boron metasomatic phenomena or as the result of recrystallization of detrital grains from siliciclastic sediments.

TM1 and TM2 consist of zoned crystals coming from granitic pegmatites of the ore deposits of California (Pala pegmatite district, San Diego County, California [3]) and (Pegmatite Province, Northeastern Brazil [4]), respectively.

IV. RESULTS AND DISCUSSION

The analyzed TMs samples are represented by reddish-purplish (TM1) and dark-green (TM2) in color tourmalines. These, being rich in inclusions, are classified as type III gemstones with a cabochon (for TM1) and a convex octagonal (for TM2) cut (see Fig. 1). The TMs samples occur as striated prismatic crystals showing a late fracture system arranged parallel to the hexagonal basal planes {0001} and orthogonal to the striated prisms.

μ-Raman spectra of TMs samples in the range between 200 and 1200 cm^{-1} are shown in Fig. 2.

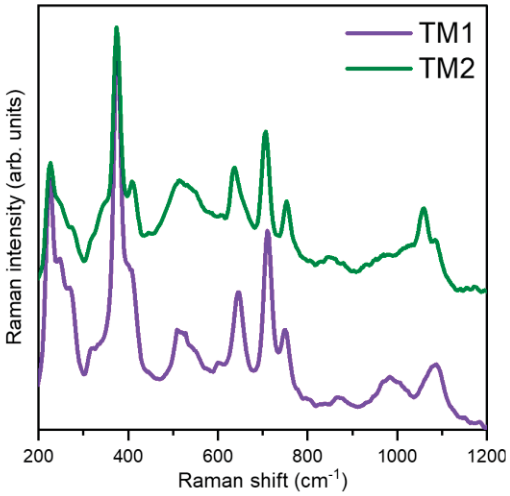

Fig. 2. μ-Raman spectra (vertically offset for clarity) of the investigated tourmaline samples.

An overall inspection of Fig. 2 reveals that both μ-Raman profiles appear quite similar, suggesting that both gemstones share a similar molecular composition and basic crystal structure. Differences are detected in the 900 – 1200 cm^{-1} spectral region, including features originating from SiO_4–ring modes and R–O (with R = Si, B) stretching vibrations, respectively.

The detected μ-Raman profiles revealed, as the main feature, two high-intense ring deformation stretching peaks of the X–O type (X: Na^{1+}, Ca^{2+}, K^{1+}, Pb^{2+}), respectively centered at ~ 229 cm^{-1} and ~ 375 cm^{-1}, together with broadband at 420 – 600 cm^{-1} due to Al–O and Y–O bond stretching vibrations (Y: Mg^{2+}, Fe^{2+}, Fe^{3+}). The well-visible triplet of sharp peaks, respectively centered at ~645 cm^{-1}, ~707 cm^{-1} and ~749 cm^{-1}, can be ascribed to multi-mode symmetrical Si–O–Si vibrations of individual $[Si_6O_{18}]^{12-}$ rings. In particular, the contribution falling at ~ 645 cm^{-1} accounts for the Si–O rocking mode involving *bridging* oxygens (O_{br}) of the ring (that link two SiO_4 tetrahedra), whereas the ~ 707 cm^{-1} and ~ 749 cm^{-1} contributions respectively arise from the "breathing" mode of O_{br} in $[Si_6O_{18}]^{12-}$ and the Si–O–Si bending. Finally, all spectral features falling within the 920 – 1200 cm^{-1} range involve the $[BO_3]^{3-}$ structural unit, including the B–O stretching and the BO_3 deformation, as well as the Al–O stretching and AlO_6 deformations [5-15].

Based on the assignment above, both the investigated samples turn out to be *elbaitic*-type TMs, presumably of magmatic-hydrothermal origin, thus belonging to the sub-group of the alkali-species (X: Na) with idealized chemical formula $NaLi_{1.5}Al_{1.5}Al_6Si_6O_{18}(BO_3)_3(OH)_3(OH)$. This finding is supported by the fact that the TMs mines both in California (Pala) (in the case of TM1) and Brazil (in the case of TM2) constitute important providers of *elbaitic*-TM species worldwide. Worth of note, that the slight differences in the μ-Raman spectra observed for TM1 and TM2, especially in the 900 – 1200 cm^{-1} wavenumber region (see figure 2), should be ascribed to the occurrence of different cation substitution processes involving end-member groups of the *elbaitic*-type TM unit, most likely due to a difference in the gemstone growth geological background.

Moreover, an elemental analysis through XRF was carried out to identify the chromophore element responsible for the color in TM1 and TM2 gemstones. The obtained elemental composition is summarized in Table 1, whereas the obtained spectra are reported in Fig. 3.

Table 1. Elemental composition of the analyzed tourmalines, as obtained by XRF data.

Sample ID	XRF elemental composition
TM1	S, Mn, Ca, K, Sn, Pb, Fe, Zn
TM2	Fe, Mn, Ca, Zn, K, Pb, Sn

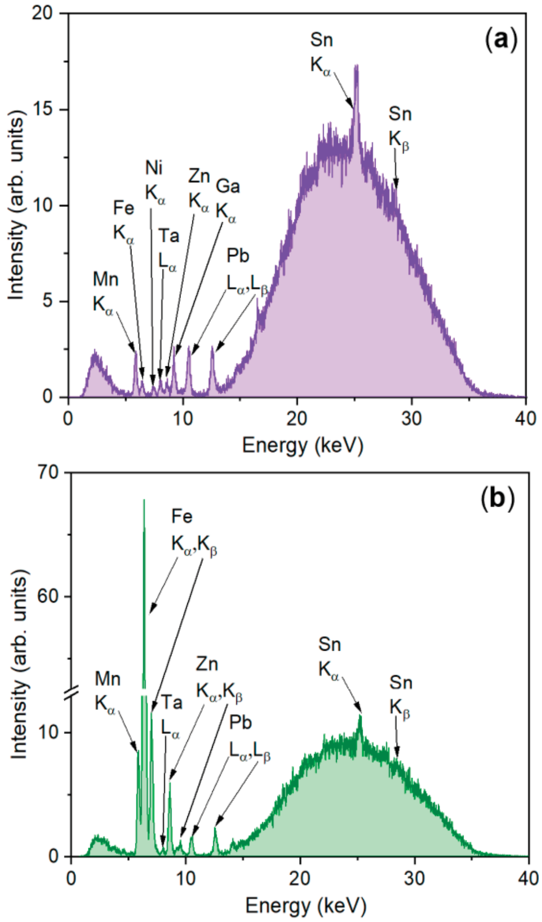

Fig. 3. XRF spectra, in the 0–40 keV range, of TM1 (a) and TM2 (b).

It is worth underlining that all major components of the *elbaitic*-type TM chemical structure (Na, Li, Al, Si, B) are characterized by a low Z number (< 15). Hence, they cannot be detected by XRF analyses. Generally, the color in natural tourmalines can be correlated to the presence of Mn (Mn^{2+}, Mn^{3+}), Fe (Fe^{2+}, Fe^{3+}), and Ti (Ti^{4+}) elements within the Y-site of the TM unit or to the existence of impurity defects and charge transfer between cations. In the case of the TM1 sample, a high concentration of Mn with respect to other elements (see Table 1) indicates that the observed reddish coloration can be reasonably attributed, in agreement with what was already reported in the literature [16], to the presence of Mn atoms occupying the Y sites of the crystal structure, following Mn ↔ [$Li_{1.5}Al_{1.5}$] end-member substitutions. In this case, the more violetish color of TM1 suggests a gradual conversion of Mn^{2+} into Mn^{3+}, consequently a prolonged exposure to natural radiation. In addition, small amounts of Ca, K, Sn, Pb, Fe, and Zn were also observed.

In the case of TM2, a higher amount of Fe with respect to that observed in TM1 was observed, together with traces of other elements such as Mn, Ca, Zn, K, Pb, and Sn. Such circumstance identifies Fe as primarily responsible for the dark-green hues observed under the stereomicroscope, in agreement with what was found in [17]. More in detail, the obtained elemental composition suggests the existence of color centers mainly based on Fe (Fe^{2+}) and, to a lesser extent, on Mn (Mn^{2+}) atoms, spatially arranged in octahedral coordination within the Y- and Z-site of the TM unit, respectively. Finally, although both Mn and Fe are observed in the elemental compositions of the investigated gemstones (see Table 1), the Mn/(Fe+Mn) and Fe/(Mn+Fe) ratios calculated for TM1 (0.96 and 0.03, respectively) and TM2 (0.14 and 0.85, respectively) testifies how such elements are individually responsible for the reddish-pinkish (Mn) and dark-green (Fe) colors observed in TM1 and TM2 (commercially known as *rubellite* and *verdelite*, respectively), validating the XRF technique for the identification of the chromophore element in TMs samples.

V. CONCLUSIONS

A preliminary investigation was carried out on two different colored TMs coming from the granitic pegmatites of California (Pala) and Brazil through μ-Raman, and XRF combined sensitive techniques to obtain mineral "fingerprinting". The molecular and elemental composition obtained by μ-Raman and XRF spectroscopies, respectively, allowed to classify the investigated gemstones as *elbaitic*-type tourmalines originating from magmatic-hydrothermal fluids and to unambiguously identify the chromophore elements responsible for the observed colorations. This study could represent, in principle, a starting point for the classification of different unknown tourmaline species of different provenance. In the light of this, to sustain the effectiveness of the used approach, comparisons with other samples of known provenance will be subject of forthcoming investigations.

REFERENCES

[1] P.G. Manning, "An optical absorption study of the origin of colour and pleochroism in pink and brown tourmalines", Canad. Mineral., vol.9, No.5, June 1969, pp.678-690.

[2] W A Deer, Howie R A and Zussman J 2013 Mineralogical Society of Great Britain and Ireland, DOI: https://doi.org/10.1180/DHZ, ISBN electronic: 9780903056434, ISBN print: 9780903056274.

[3] Novák M and Taylor M C 2000 *The Canadian Mineralogist* 38 (6) 1399–1408.

[4] Thais Andressa CarrinoSandra de Brito BarretoPaula Jussara Azevedo de OliveiraJosé Ferreira de Araújo NetoAldine Maria de Lima Correia 2019 *Braz. J. Geol.* 49 (02).

[5] L.H. Hoang, N.T.M. Hien, X.B. Chen, N.V. Minh, I.-S. Yang, "Raman spectroscopic study of various types of tourmalines", J. Raman Spectrosc., vol.42, No.6, June 2011, pp.1442-1446.

[6] B. Gullu, Y.K. Kadioglu, "Use of tourmaline as a potential petrogenetic indicator in the determination of host magma: CRS, XRD and PED-XRF methods", Spectrochim. Acta A Mol. Biomol. Spectrosc., vol.183, August 2017, pp.68-74.

[7] K. A. Musiyachenko, A. V. Korsakov, R. Shimizu, P. S. Zelenovskiy, and V. Y. Shur, "New insights on Raman spectrum of K‐bearing tourmaline," J. Raman Spectrosc., vol. 51, no. 9, Sep. 2020, pp. 1415‐1424.

[8] A. Watenphul, M. Burgdorf, J. Schlüter, I. Horn, T. Malcherek, and B. Mihailova, "Exploring the potential of Raman spectroscopy for crystallochemical analyses of complex hydrous silicates: II. Tourmalines," Am. Mineral., vol. 101, no. 4, Apr. 2016, pp. 970–985.

[9] A. Culka and J. Jehlička, "A database of Raman spectra of precious gemstones and minerals used as cut gems obtained using portable sequentially shifted excitation Raman spectrometer," J. Raman Spectrosc., vol. 50, no. 2, Feb. 2019, pp. 262–280.

[10] C. Fantini, M. C. Tavares, K. Krambrock, R. L. Moreira, and A. Righi, "Raman and infrared study of hydroxyl sites in natural uvite, fluor-uvite, magnesio-foitite, dravite and elbaite tourmalines," Phys. Chem. Miner., vol. 41, no. 4, Apr. 2014, pp. 247–254.

[11] C. Castañeda, S. G. Eeckhout, G. M. da Costa, N. F. Botelho, and E. De Grave, "Effect of heat treatment on tourmaline from Brazil," Phys. Chem. Miner., vol. 33, no. 3, May 2006, pp. 207–216.

[12] A. Watenphul, T. Malcherek, F. D. H. Wilke, J. Schlüter, and B. Mihailova, "Composition–thermal expandability relations and oxidation processes in tourmaline studied by in situ Raman spectroscopy," Phys. Chem. Miner., vol. 44, no. 10, Nov. 2017, pp. 735–748.

[13] C. Zhao, L. Liao, Z. Xia, and X. Sun, "Temperature-

dependent Raman and infrared spectroscopy study on iron–magnesium tourmalines with different Fe content," Vib. Spectrosc., vol. 62, Sep. 2012, pp. 28–34.

[14] L. X. Fu, Y. Guo, Q. H. Zhang, J. Huang, and L. J. Wang, "Tourmaline@ZnO Core–Shell Structural Composites: Fabrication, Characterization, and Optical Properties," J. Electron. Mater., vol. 47, no. 8, Aug. 2018, pp. 4289–4295.

[15] B. J. Reddy, R. L. Frost, W. N. Martens, D. L. Wain, and J. T. Kloprogge, "Spectroscopic characterization of Mn-rich tourmalines," Vib. Spectrosc., vol. 44, no. 1, May 2007, pp. 42–49.

[16] F.S. da Silva, M.A. Moura, H. de A. Queiroz, J.D. Ardisson, "Chemical and spectroscopic characterization of tourmalines from the Mata Azul pegmatitic field, Central Brazil", J. Geosci., vol.63, No.2, July 2018, pp.155-165.

[17] X. Liu, X. Feng, J. Fan, S. Guo, "Optical absorption spectra of tourmaline crystals from Altay, China", Chin. Opt. Lett., vol.9, No. 8, August 2011, pp. 083001-083001.